Materials Science and Engineering C 78 (2017) 79–87

Contents lists available at ScienceDirect

Materials Science and Engineering C

journal homepage: www.elsevier.com/locate/msec

On mechanical mechanism of damage evolution in articular cartilage

Yu-tao Men *, Yan-long Jiang, Ling Chen, Chun-qiu Zhang *, Jin-duo Ye

Tianjin Key Laboratory of the Design and Intelligent Control of the Advanced Mechatronical System, PR China

ARTICLE INFO

Article history:
Received 2 August 2016
Received in revised form 20 December 2016
Accepted 30 March 2017
Available online 1 April 2017

Keywords:
Biological materials
Damage mechanics
Cartilage
Crack
Numerical analysis

ABSTRACT

Superficial lesions of cartilage are the direct indication of osteoarthritis. To investigate the mechanical mechanism of cartilage with micro-defect under external loading, a new plain strain numerical model with micro-defect was proposed and damage evolution progression in cartilage over time has been simulated, the parameter were studied including load style, velocity of load and degree of damage. The new model consists of the hierarchical structure of cartilage and depth-dependent arched fibers. The numerical results have shown that not only damage of the cartilage altered the distribution of the stress but also matrix and fiber had distinct roles in affecting cartilage damage, and damage in either matrix or fiber could promote each other. It has been found that the superficial cracks in cartilage spread preferentially along the tangent direction of the fibers. It is the arched distribution form of fibers that affects the crack spread of cartilage, which has been verified by experiment. During the process of damage evolution, its extension direction and velocity varied constantly with the damage degree. The rolling load could cause larger stress and strain than sliding load. Strain values of the matrix initially increased and then decreased gradually with the increase of velocity, and velocity had a greater effect on matrix than fibers. Damage increased steadily before reaching 50%, sharply within 50 to 85%, and smoothly and slowly after 85%. The finding of the paper may help to understand the mechanical mechanism why the cracks in cartilage spread preferentially along the tangent direction of the fibers.

1. Introduction

Articular cartilage is a biological material consisting of a solid phase extracellular matrix and a porous liquid phase. The extracellular matrix mainly consists of proteoglycans that are reinforced by a tension-resistant fiber network [1]. A unique mechanical property of the extracellular matrix is its ability effectively resist joint impact force with reduced friction and wear between joints [2–4]. However articular cartilage is in frequent use, which generates chronic mechanical stress. For example, knee joint cartilage is susceptible to injury due to the mechanical stress. Moreover, impaired articular cartilage commonly accompanied by increased joint mechanical stress is suggested to contribute to degenerative osteoarthritis [5–7]. If articular cartilage is damaged, repair to pre-injury levels is challenging [8,9]. Thus, it is important to understand processes related to injury susceptibility and/or pathophysiology of diseases associated with damaged articular cartilage.

In our previous experiments, crack propagation of cartilage did not follow the normal direction of the boundary, but follow the direction of an angle with normal (Fig. 1). There was a branch at the tip of the split. The crack direction observed wasn't always straight forward, but changed constantly at the different layer of the cartilage. The phenomenon of the experiment could not be explained at that time. It is important to understand damage evolution mechanism of cartilage for curing cartilage injury diseases. We hypothesized that the filbers of the cartilage may affect the crack propagation of damage cartilage and the process of the damage evolution of the cartilage.

To date, there have been some studies on mechanical mechanism of damaged AC. Thambyah et al. [10] studied the failure of AC following creep loading induced by impact load with fracture mechanics method. They found the creep-loaded cartilage matrix exhibited a substantial radial collapse or compaction of the fibrillar network in its primary radial zone. The increase of crack length in the prior creep-loaded cartilage was consistent with a reduction in its dissipative properties as indicated by a reduction in rebound velocity. Hosseini et al. [11] established the finite element composite model of cartilage matrix and collagen, their study found that the matrix damage and fiber fracture had different impact on the cartilage damage progress. Ground substance softening and collagen damage had distinct effects on cartilage mechanopathology, and damage in either one of them may promote each other. Kaplan [12] performed a study on the mechanical fatigue of cartilage with the test of healthy human tissue in vivo. Research indicated there was progressively more damage to the microstructure of matrix and collagen network under the 20 N 1.44 Hz through 200 N 2.88 Hz loading. There was significant physical damage under the higher loading conditions, particularly 200 N at 2.88 Hz. Kenneth [13] found defect presence had dramatic effects on dynamic cartilage deformation and defects district

* Corresponding authors at: School of Mechanical Engineering, Tianjin University of Technology, Tianjin 300384, PR China.
E-mail address: yutaomen@163.com (Y. Men).

http://dx.doi.org/10.1016/j.msec.2017.03.289
0928-4931/

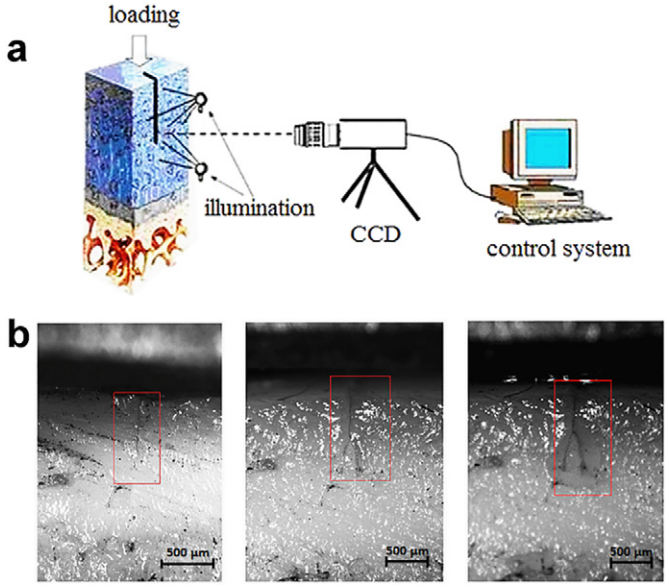

Fig. 1. Schematic diagram of experimental system under rolling and sliding loads (a), the experimental images (b) of crack extension direction in different time.

affected strain distributions markedly. Tissue adjacent to a defect experienced increased magnitudes of axial, lateral, and shear strain. These studies demonstrated that as damage to the articular cartilage progresses, more severe immediate and adjacent structural consequences occur such as fibrillation and deep cracks penetrating into soft tissue. These and other maladaptations are impactful activities of daily living because they contribute to reduced tissue stiffness [14] under tension, which is paralleled by increased compression and shear stress [15–18] followed by gradual decreases in cartilage carry capacity [19]. Lastly, although the exact responsible mechanisms remain unclear, several histological studies have shown that chondrocyte death is a maladaptive response to exacerbated mechanical loading of cartilage [20–23]. In addition, the tissue engineering repair therapy is closely related to the mechanical environment in damage zone [24–26]. The primary aim of this study was to assess the mechanical mechanism of cartilage damage evolution using a fiber-reinforced viscoelastic finite element model with profound consideration of the hierarchical structure and fiber distribution characteristics of cartilage. With these data, we aim to demonstrate a new model that will be able to predict the cartilage response to damage under several loading conditions.

2. Materials and methods

2.1. Cartilage finite element model

ANSYS 12.0 was used to establish 2D fiber-reinforced finite element model [16,20,27,28]. Illustrated in Fig. 2, the cartilage model (6 mm long, 2 mm thick) was divided into surface (10%), middle (40%) and deep layers (50%). The plane183 elements for the matrix and link1 elements for the fibrils were chosen. The viscoelastic response of the matrix was taken into account in this study. Relaxation modulus was

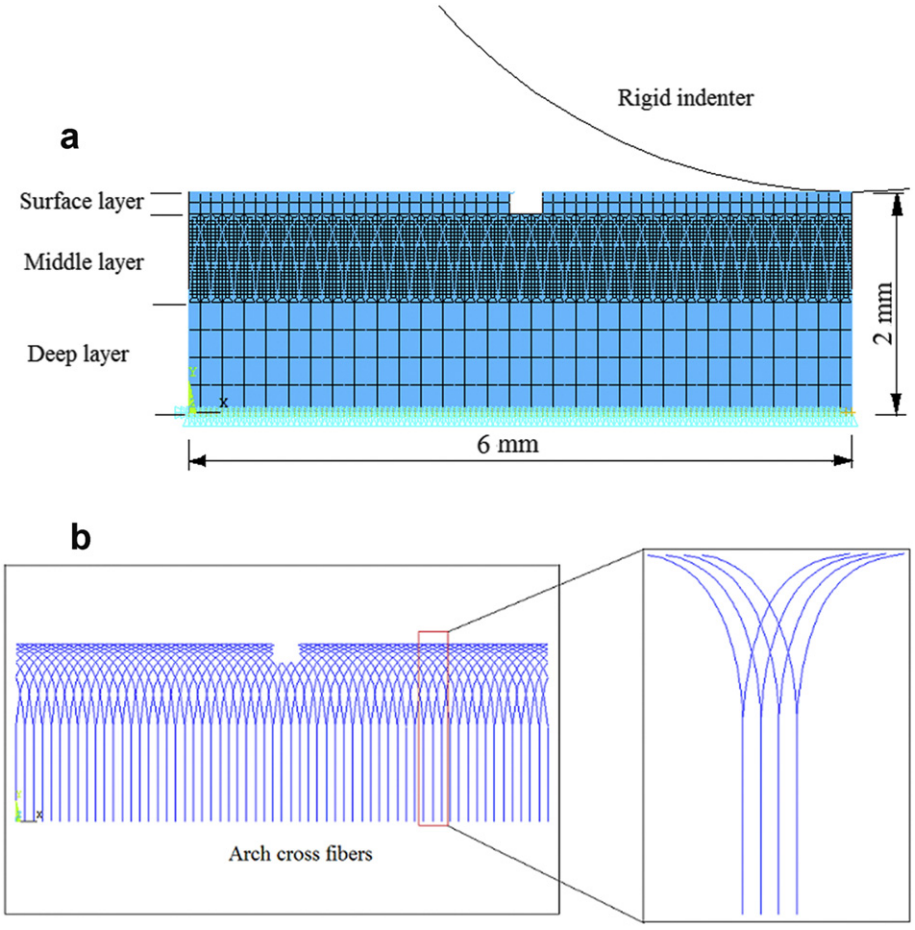

Fig. 2. The cartilage model (6 mm long, 2 mm thick) was divided into surface, middle and deep layers. The matrix chose plane strain quadrilateral elements with 8-node and the fibrils chose the link elements (a). The fiber orientation of the surface layer was nearly parallel with the upper surface layer (0° to 30°), the middle fibers crossed each other (30° to 90°), and the deep fibers were perpendicular to the subchondral bone (90°) (b).

fitting and calculated according to data of the creep experiments in the study team. Relaxation modulus E (t) using Prony series was expressed as:

$$E(t) = 0.95 + 0.23e^{\frac{-t}{71.1}} + 0.28e^{\frac{-t}{40.7}} + 0.034e^{\frac{-t}{378.2}} \quad (MPa) \tag{1}$$

As recommended from the literature [29,30], fibrils applied arcade model and their orientation changed as a function of depth. Briefly, the fiber orientation of the surface layer was nearly parallel with the upper surface layer (0° to 30°), the middle fibers crossed each other (30° to 90°), and the deep fibers were perpendicular to the subchondral bone (90°) (Fig. 2b). The fibers that the cross-sectional diameter was $2e^{-5}$ mm [20] were embedded in matrix by common nodes. There was a rigid roller (R5 mm) above the cartilage. The interface applied contact elements and the friction coefficient 0.05 between the indenter and cartilage. There was a preformed defect (0.3 mm wide, 0.2 mm deep) in the upper part of cartilage model. The bottom was fixed, and the roller was applied by rolling or sliding load respectively. Load boundary conditions were imposed on the rigid roller: step1 was to apply downward displacement; step2 was to apply linear velocity v and angular velocity ω, determined based on the relation $\omega = \frac{v}{R}$. For example, in the numerical simulation, downward displacement $u_y = 0.2$ mm, velocity $v = 20$mm/s, angular velocity for rolling load $\omega = 4$ rad/s and angular velocity for sliding load $\omega = 0$.

The material parameters of the simulated cartilage are presented in Table 1. Damage and evolution of the cartilage matrix and fibers were simulated with the command of "birth and death" element.

2.2. Damage evolution criterion

The cartilage was modeled as a fiber-reinforced material. Therefore, the progression of cartilage damage was represented by a gradual failure process of composite material [30], which includes matrix damage and fiber fracture. Because of the complex nature of cartilage damage, the maximum strain theory was applied as our criterion [11]. Accordingly, if the equivalent strain of cartilage matrix exceeds a specific threshold, we suggest that this eventually leads to cell necrosis and reduced stiffness. Similarly, if the equivalent strain of fiber exceeds a specific threshold, then we could expect to observe fiber lose efficacy and decreased stiffness. Thus, as model loading cycles accumulate, fiber and matrix stiffness should reduce to zero.

Equivalent strain of collagen fibers, as shown in formula (2):

$$\varepsilon_{eq.f} = \varepsilon\left(\vec{x}\right) \tag{2}$$

Equivalent strain of cartilage matrix, as shown in formula (3):

$$\varepsilon_{eq,m} = \frac{1}{3}\sqrt{2\left[(\varepsilon_1-\varepsilon_2)^2 + (\varepsilon_1-\varepsilon_3)^2 + (\varepsilon_2-\varepsilon_3)^2\right]} \tag{3}$$

where $\varepsilon_i (i = 1,2,3)$ are principal strain of matrix in three directions, as shown in formulas (4) and (5):

$$K = \sum \delta k_i \tag{4}$$

$$\delta = \begin{cases} 1 & if \quad \varepsilon_{eq,i} < \varepsilon_{\max,i} \\ 0 & if \quad \varepsilon_{eq,i} \geq \varepsilon_{\max,i} \end{cases} \tag{5}$$

Table 1
Materials parameters of cartilage [29].

Cartilage layer	Young's modulus E(MPa)	Poisson's ratio ν
Surface layer	0.35	0.11
Middle layer	0.78	0.15
Deep layer	1.32	0.17
Fiber	10	0.22

where K is the whole matrix stiffness of cartilage matrix or fiber, k_i are element matrix stiffness of cartilage matrix or fiber.

To show the process of evolution, the command "birth and death" was used. According to damage evolution criterion, the region of maximum equivalent strain is vulnerable to damage. When the maximum equivalent strain was reached the failure threshold during computation, the elements were deleted. It is hard to find the accurate value of strain thresholds. The strain thresholds used in the numerical simulation according to the results of experiment. The boundary conditions include the magnitude of load and the velocity of the roller could be recorded by instruments when the crack spread had been observed in experiment, the same boundary conditions had been applied to the numerical model and the strain thresholds could be determined by numerical simulation. The strain failure threshold was 0.25 in this model. It is found that the strain threshold was not a constant and decreased with evolution steps. In this study, the material damage behaved as failure caused by fatigue loads, the maximum equivalent strain might be less than the failure threshold in cartilage. If the maximum equivalent strain reached the over 95% of the maximum value, the element was deleted on behalf of material failure. If the maximum equivalent strain reached a range from 90% to 95% of the maximum value, the element was not deleted, but the stiffness coefficient of element was set at 0.8 on the behalf of material softening. Each evolution step included 20 load cycles. The stiffness coefficient of element was reset at each evolution step. Although the N-th damage extension didn't represent a true evolution number, this could be used as a description of the extension trend.

3. Results

3.1. The process of cartilage damage evolution

To study the process of cartilage damage evolution, rolling load was applied and four strain contours in different damage extension period were selected, as shown in Fig. 3. Because there was no direct load on the middle portion of defect gap, the strain at this location was small and the damage process was extremely slow, where a bump "isolated island" was form.

The process of fiber damage evolution corresponding to the cartilage matrix is shown (Fig. 3 right). The fibers in the shallow surface mainly bear tensile stress [31]. With exacerbating damage, the stress superficial fibers turned gradually from tensile stress into compressive stress leading to loss of bearing capacity by the superficial fiber network. Although a portion of compressive stress was transmitted to middle and deep fibers, maximum values appeared on fibers at the bottom corners.

3.2. The effect of load forms on damage evolution

After the first time loading, strain contours were obtained (Fig. 4).

Irrespective of load, there was an obvious stress concentration on both sides of the defect region spanning to the surface layer, whereas maximum values appeared at the bottom corners of the defect. The maximum tensile strain value was 0.19 under the sliding load, while 0.23 under rolling load. However, the strain of healthy cartilage at the same location was approximately 0.05 and 0.06, respectively. The equivalent strain in the defect area edge was approximately four times greater than strain of normal cartilage at the same location under the same pressure.

In Fig. 5 (a) there was a trend for variation of maximum equivalent strain to accumulate damage extension for 10 times under rolling and sliding load. Illustrated in Fig. 5 (a), with increasing damage, the equivalent strain in the defect area initially increased briefly. Subsequently, the values decreased gradually until they were almost equal. However, during this extension process, numerical values under rolling were

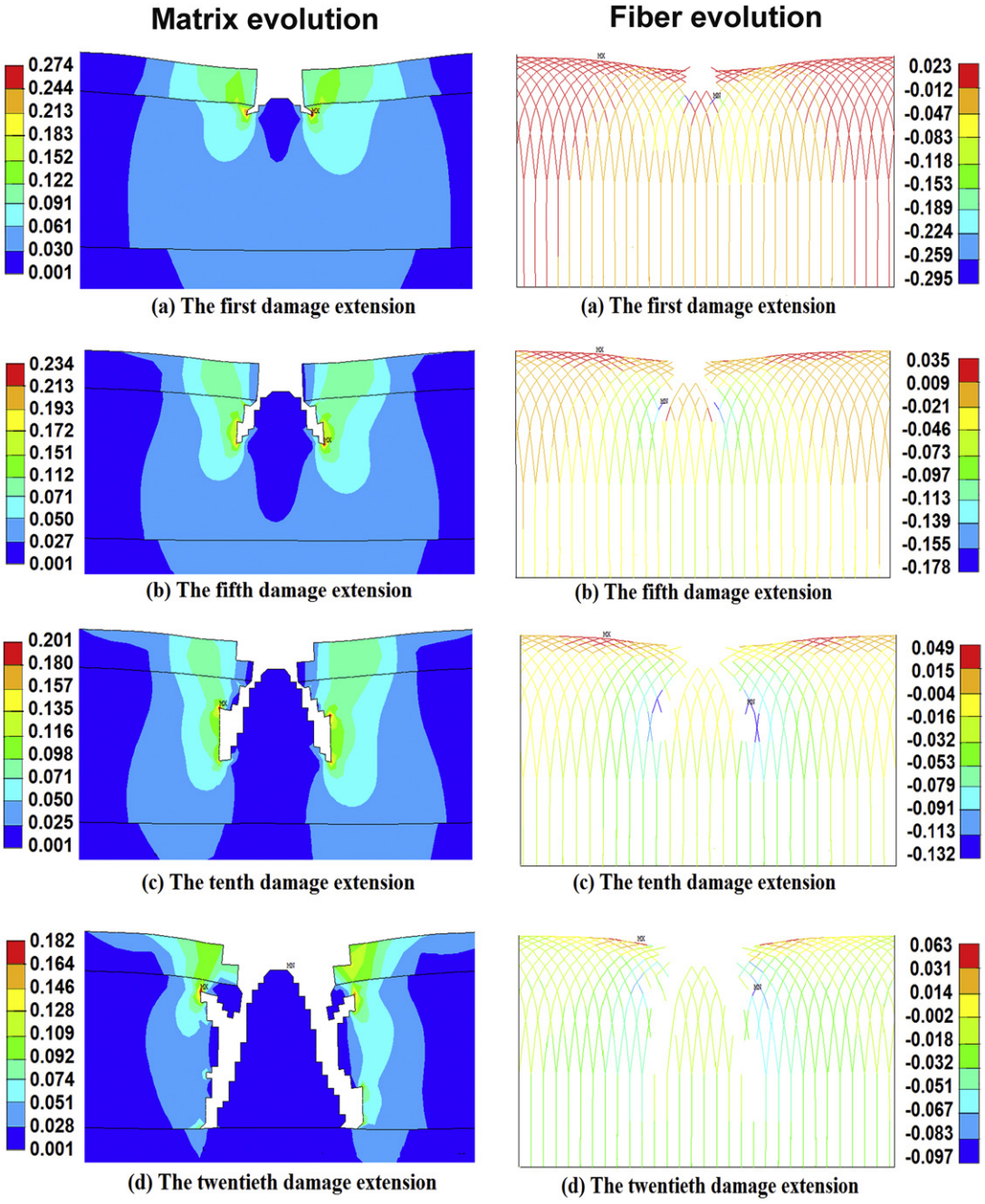

Fig. 3. The equivalent strain contours of matrix evolution (left) and the axial strain contours of fiber evolution (right). The position of roller was above the gap. The micro-defect cartilage began to damage at the bottom corners of the defect (left a) while gradually extending into deeper cartilage imposed by the loading conditions, which led to a continual expansion of the defect gap (left b,c,d); When damage of the matrix was close to the deep layer, cartilage cracking gradually extended along boundary layers between the surface and middle sections at the same time (left d).

consistently higher than sliding. Thus, the rolling load was able to generate greater stress and strain on the cartilage compared to the sliding load.

In order to further study the stress distribution regularity in different position under two kinds of loads, 10 stress points at the bottom and right side of the defect edge were extracted after the fifth damage evolution (Fig. 5 (b)). Presented in Fig. 5 (c) and (d), Horizontal stress values were less than the vertical on the defect edge, which illustrated that the load had a greater effect on the vertical direction. Around the defect area, the maximum stress value under rolling was always greater than sliding. Cumulatively, the cartilage damage evolution under rolling load was faster than sliding load and the former had more influence on cartilage damage than the latter.

3.3. The effect of velocity on damage evolution

Based on the actual movement velocity [32], four different rolling velocities were selected, and the equivalent strain values with the variation of roller displacement around bottom corner (point 5 in Fig. 5(b)) were extracted (Fig. 6(a)).

Shown in Fig. 6(a), when the roller was located in the non-damaged region of both sides, all strains were approximately 0.03 under four different rolling velocities, demonstrating minor fluctuations as the defect gap was approached. When the roller was located above the gap, strain reached to maximum values. With the increase of velocity, the strain initially increased and then decreased.

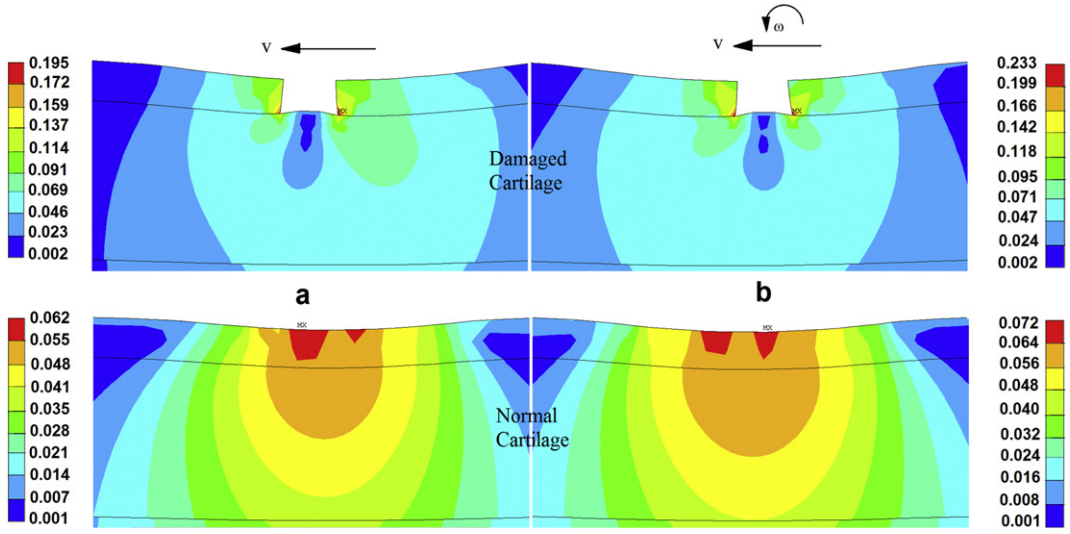

Fig. 4. The equivalent strain of damaged and normal cartilage under sliding (a) and rolling (b) load. First force causing 0.15 mm displacement was applied downward in the center of roller, which was followed by 50 mm/s tangential and 10 rad/s angular velocity loading, and then sliding without angular velocity loading.

This study suggested that with increased velocities causing short contact time between roller and cartilage, cartilage deformation was small and stress could not accumulate. Also, the friction forces of cartilage on upper surfaces decreased modestly with increasing rolling velocity [33]. As can be seen from Fig. 6 (b), the change of fiber's tensile stress and compressive stress under different velocities was not obvious, except for increasing slightly in the 20 mm/s. The maximum tensile stress and compressive stress of fiber almost decreased with the increase of velocity. On the whole, the velocity just had a slight influence on the damage evolution of the fiber. The higher velocity was the faster

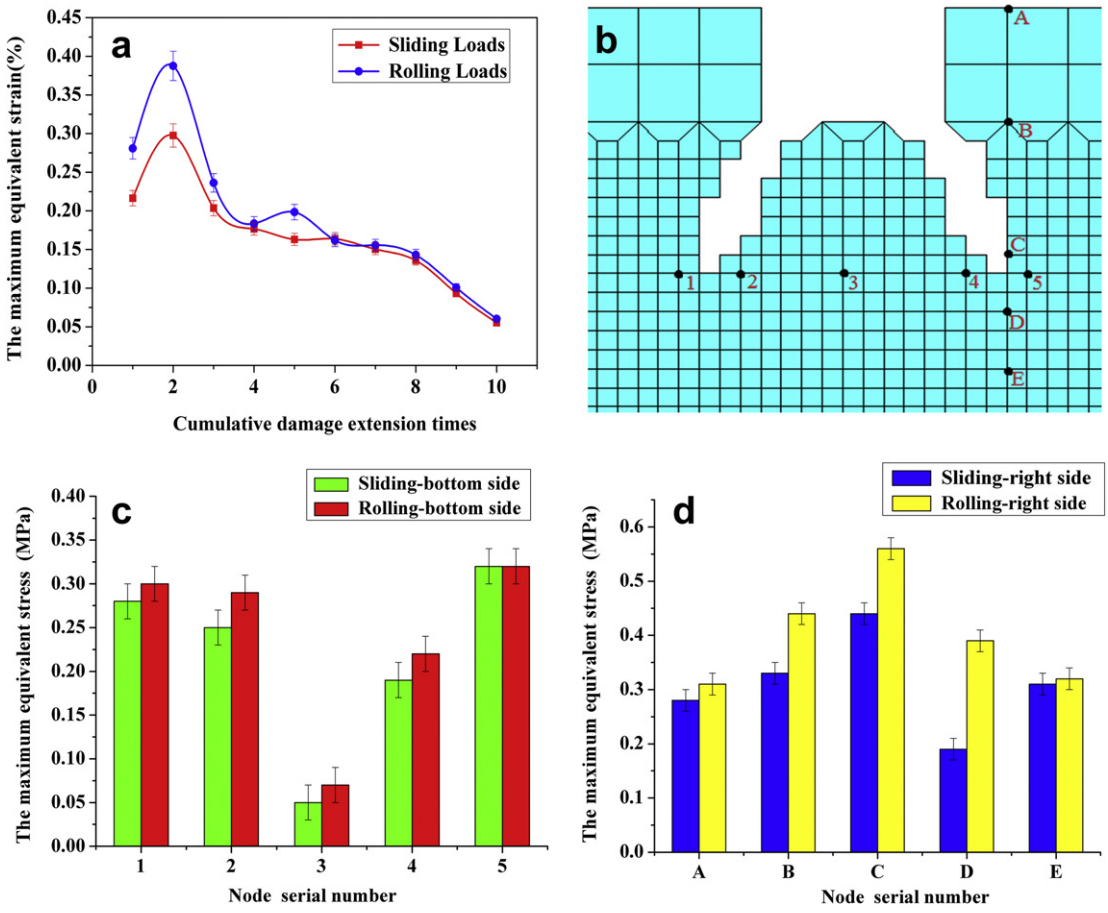

Fig. 5. Curve of equivalent strain under different loads (a), the maximum value reached 0.38 under rolling, whereas the sliding value of 0.28 was slightly lower than rolling; locations of the stress points (b); variation of equivalent stress in different nodes of defect bottom side (c) and defect right side (d), the closer distance was from the defect edge, the larger the stress value and the faster the damage extend.

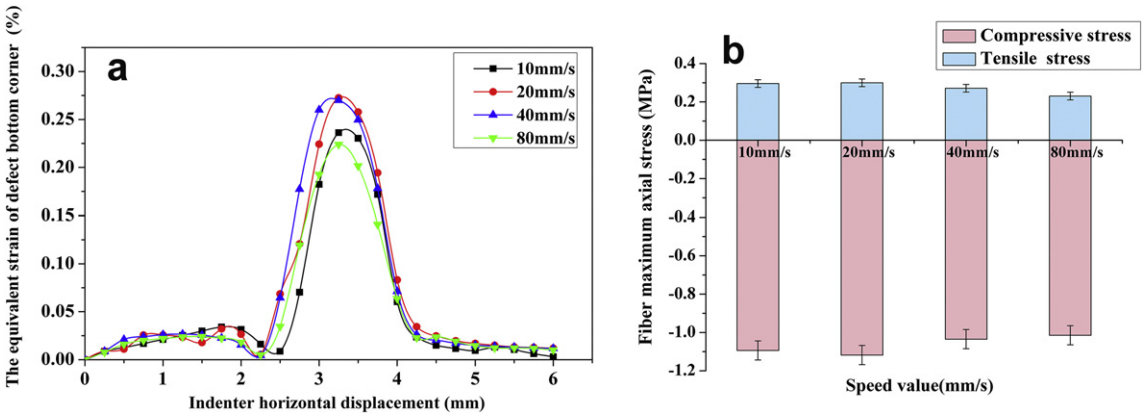

Fig. 6. Curve of equivalent strain (a) and the axial stress (b) of fiber in different speed rates. The location of the defect is in the range of 3 to 3.5 mm.

and more serious cartilage damage evolution. The velocity had a greater effect on cartilage matrix than fibers network. It was consistent with the conclusion in the literatures [34].

4. Discussion

Because of slow damaging processes, it is challenging to observe the process of articular cartilage in vivo. This study presented an articular cartilage damage progression model, which was based on established composition-based cartilage mechanical modeling. Considering the important role of collagen fiber in adjusting stress distribution and limiting lateral deformation, a new fibril structure was specifically created from the assumption of Wilson [9,35] in this study. Wilson presented the depth-dependent arcade fibril structure, and primary fibril directions extended perpendicular from the subchondral bone, splitting up close to the articular surface into fibrils which curve to a horizontal course, flush with the articular surface. Later, he demonstrated the validity of this structure by means of related experiment. Based on his research, A 2D fiber-reinforced composite model [36] was established in this paper. The viscoelastic [34,37] and nonlinear characteristic [14,38,39] of the matrix were considered in this model. The fiber network distribution of the model was depth-dependent arch structure. There were some similar models in the literature. We selected several representative models to compare and analyze carefully. There was no collagen fiber network in some models [13,36,40,41]. Although some models contained fiber network, the structure distribution of fiber was not depth-dependent arch structure, just replaced with spring elements [11,42–44]. Some models weren't given the viscoelastic property or the viscoelasticity was replaced with hyperelasticity or elastoplasticity [30,36,38,45–47]. Besides, some models were applied unidirectional compression load rather than rolling and sliding loads in the simulation [27,48,49]. Our model didn't contain osmotic pressure and secondary fibers, but it can be found that the simulate results compare well with the results of other FE studies [11,13]. This articular cartilage damage model can predict damage development of the cartilage matrix and fiber network under several conditions of mechanical loading.

These results show regularities in the process of damage evolution, which is mainly reflected in the extension direction and velocity. The process of cartilage damage extension demonstrates a close relationship with the disruption of fiber network, while the damage of cartilage matrix and fibers parallel one another [11]. Y. Al-Saffar et al. [50] did experiments and found that the role of these oblique fibers was emphasized in supporting compressive loads. The SEM images also proved that the direction of cracks propagation was associated with the distribution structure of fibers [10]. The direction of cracks propagation in simulation is consistent with their experiments.

We show in this study, damage cases comparing fibers and no fibers in the early period of cartilage damage (Fig. 7 (a) (b)). This study demonstrates that if there are no fibers in the model, the cartilage matrix in shallow surfaces bears greater strain leading to damage which primarily extends to both sides of the gap. In contrast, in the model containing the fibrous network, the damage of cartilage matrix roughly extended down along the fiber in the tangent direction, which was paralleled by a smaller surface layer strain. The fiber seems to play a "guide" role in cartilage damage evolution. In fact, there has been similar report that cartilage damage, observed during axial indentation, is expressed in the form of cracks on the cartilage surface in the middle of the impact area, which then propagates downward at approximately 45 degrees [10,45,51]. Simulation results in our study qualitatively agree with the above mentioned damage patterns.

As previously stated, it is challenging to directly study damage evolution velocity. Thus, this paper firstly discussed the distance of damage extension in different directions with the aid of the model. We assume that after the N-th damage extension, the maximum distance of defect gap in horizontal direction from the center line was λ_n and in vertical direction from the cartilage upper surface was δ_n. (Fig. 7(c)). We demonstrate in the Fig. 7 (d) that in the early damage extension period, the evolution velocity of the matrix gap in vertical direction occurs faster compared to the horizontal direction. However, when damage reached the deep layer, the velocity in horizontal direction accelerated quickly and exceeded the vertical direction. Thus, we predict that due to the enlargement of the defect gap and fracture of the fiber network between joint frictions, damage in the middle surface layer aggravated in the horizontal direction, which resulted in the damage area increasing rapidly. Additionally because of lacking of nutrition from the peripheral tissues [52], the "isolated island" formed in the middle gradually atrophied and died out, forming further irregular polygon or circle in the surface [53], which eventually became a pit which the edge was rugged and a part of fiber expose.

Considering differences in model sizes (in length and thickness), as well as fiber spacing and material parameters, it is inadequate to study quantitative relationships while only considering damage distance in different directions. After repeated simulation analysis, we observed that there are certain relationships between damage distance in two directions and the whole evolution depth. Moreover, when the damage reached the deep layer (about 50% of the total thickness), the velocity of damage evolution in two directions changed significantly, therefore we could use a damage parameter to describe the whole process of cartilage damage. To further study the damage law of cartilage, a damage evolution index K is defined, representing the total extent of damage evolution with the increase of depth h. Here, K is represented as:

$$K = \begin{cases} p\dfrac{2\lambda(h)}{L} + (1-p)\dfrac{\delta(h)}{H} & 0<h\le 0.5 \\ q\dfrac{2\lambda(h)}{L} + (1-q)\dfrac{\delta(h)}{H} & 0.5<h\le 1 \end{cases} \tag{6}$$

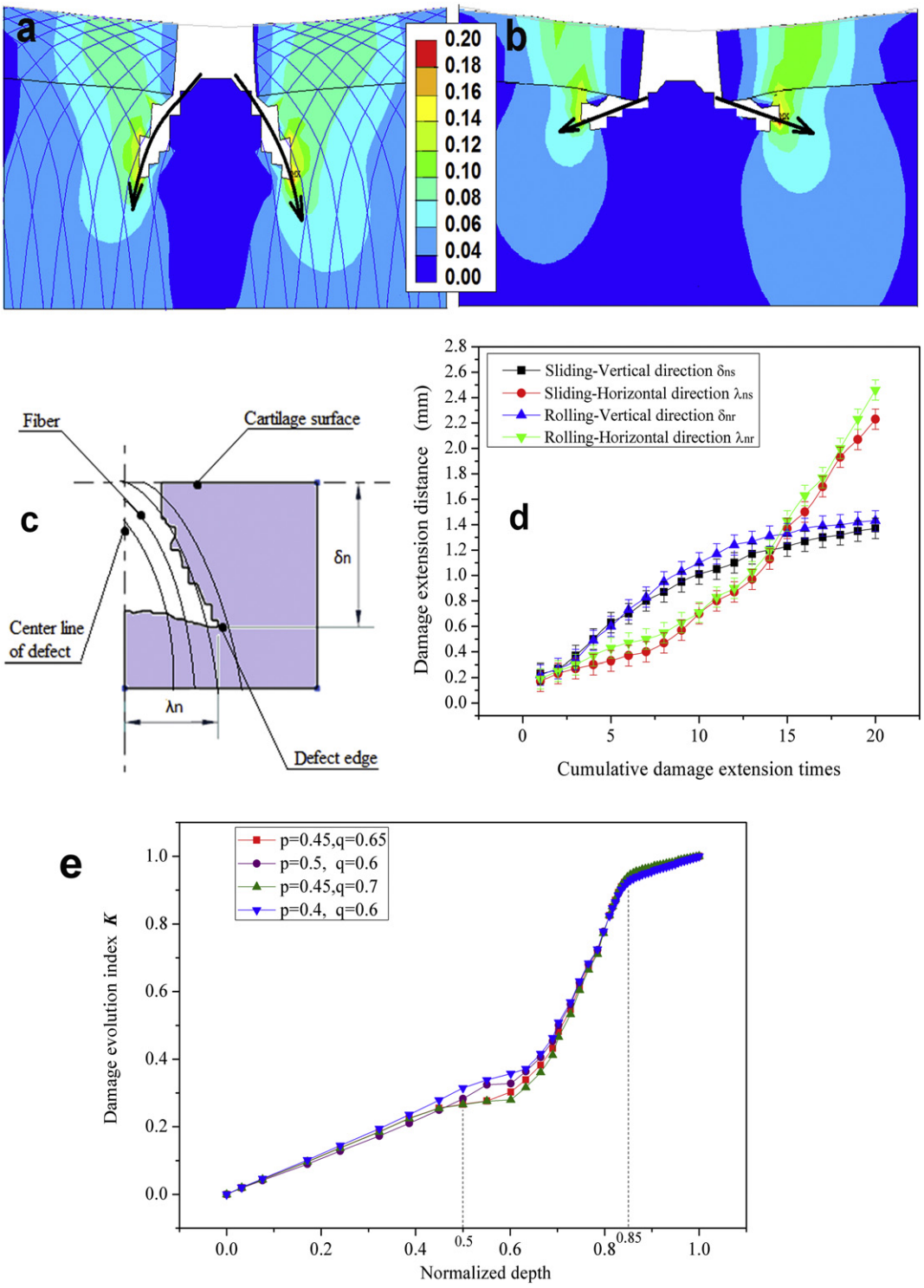

Fig. 7. The evolution direction of containing fiber (a) and no fiber (b); defect schematic diagram of cartilage (c);curve of extending distance in two directions (d) and damage evolution index variation (e).

where h is the normal depth, p and q are the weighting coefficient, $2\lambda(h)$ and $\delta(h)$ respectively represent horizontal and vertical extension distance (mm), L and H respectively represent the length and thickness of the cartilage model (mm). Considering the obvious change of damage evolution velocity in two directions, so it could be divided into two parts (shown in formula 6) to study, stipulating $p \le 0.5$, $q \ge 0.6$.

We have shown in Fig. 7 (e) that the process of damage evolution tends to speed up, which was not a simple linear change. When the evolution depth reached about total 50 to 85%, damage evolution takes place two times the change. Damage increased steadily before reaching 50%, then increased sharply within the range of 50 to 85%. Whereas the trend became smooth and increased slowly after reaching 85%. We suggest that the cause for these patterns was that the surface cartilage could still resist the extension in the early damage periods, while the damage mainly extended downward. When damage reached a certain depth, shallow cartilage lost tensile ability and then the defect gap of surface enlarged promptly, and stopped gradually until it formed larger damage in the surface layer. Thus, the variation trend in the K value

curve also suggests that the damage of surface cartilage is the most serious in the total process. In addition, S.M. Hosseini et al. [11,28] created fiber-reinforced biphasic swelling model and investigated the relationship between matrix damage and fiber damage under the compression of spherical roller. They found that softening in the ground substance was predicted to localize in the superficial and transitional zone. Collagen damage was the most prominent in the superficial zone, with more diffuse damage penetrating deeper into the tissue, resulting in adverse strain gradients. Effects were more prominent if both constituents developed damage in parallel. Although the numerical models are different in both papers, both have many similar results and conclusions, which also verified this model.

In the clinical setting, a bump may be observed in the cartilage injure region. In some instances [54], clinicians suggest that this bump may be a regeneration of injured cartilage. However, based on these data, a bump in the injured cartilage region maybe not suggest regeneration, but residue after damage. Thus, the region with a bump suggests the primary stage in the process of cartilage damage. In contrast, the region without a bump suggests late stage.

The present observations will put forward a new understanding of cartilage damage for the clinical setting. The numerical results were also consistent with the strange phenomenon of crack propagation in our previous experiments. The previous experiment was an articular cartilage sample of pig under load. The cartilage was split line patterns at 90° to the surface as the crack. Firstly, the cartilage was applied cyclic compressive load (frequency 1 Hz, amplitude 0.2 ± 0.05 mm) for 1.5 h; then rolling load (frequency 1 Hz, speed 2 mm/s, displacement 0.4 ± 0.1 mm) for 1 h; finally cyclic compressive load (frequency 1 Hz, amplitude 0.2 ± 0.05 mm) for 1.5 h. There was an interval of more than one hour between each load. These loads were as soon as possible to promote cartilage damage. Although the load type was different from the numerical model, crack propagation was preference for the tangential direction of fiber.

This study suggests that tensile properties of collagen fiber strengthened the toughness of surface cartilage. However, the damage can destroy fiber network structure, so that external force was not scattered [50], which caused local stress concentration. If the damage continued to extend, the fiber network gradually lost tensile ability. Under these circumstances, the cartilage matrix almost bears all physiological loads, which to the detriment of the patient promotes further matrix damage.

This cartilage model studied the mechanism of damage evolution only considering the mechanical effect rather than the effect of cell biological activity [55] on induced damage. Material parameters selected had slightly difference with individuals. In addition, the model didn't contain osmotic pressure and secondary fibers [13,53]. Therefore, there are some differences in accuracy with realistic cartilage. These factors will be taken into account and explored in the subsequent research.

In conclusion, the simulation results indicated that the AC damage model can explain the experiment phenomenon and describe the mechanical mechanism of damage evolution for articular cartilage. It can be used to estimate tissue regions that are at the most risk for damage due to high strains, tissue compaction, or increased sliding. Moreover, it would provide biomechanical illustrations for the organization of AC. From an engineering perspective, the mechanical mechanism of AC as a load bearing tissue would also offer beneficial insights for the advances of histopathology in general. As we known, a clear mechanical mechanism of damage evolution may elucidate the clinical pathological phenomena of damage degeneration such as osteoarthritis etc. and provide the theoretical basis for prediction and treatment of cartilage damage.

5. Conclusions

This study proposes a cartilage damage progression model to better understand injury to cartilage that is observed in the clinical and research settings. These data suggest that in the early period of damage extension, cracks and damage in cartilage extend preferentially along the tangent direction of the fiber. In contrast, strain values of the cartilage matrix initially increase and then decrease gradually with the increased velocity. Velocity had a greater effect on the cartilage matrix than the fiber network. Rolling load can cause larger stress and strain than sliding load to cartilage. Damage increased steadily before reaching 50%, then sharply within the range of 50 to 85%, then smoothly and slowly after 85%. Overall, the damage extension of cartilage is a complicated process and it has a close relationship with fibers structure, load forms, movement velocities and so on. Importantly, this study on mechanical mechanism of damage evolution provides significant reference for understanding cartilage injury in the clinical setting. Therefore this model has the potential to be used in clinical setting as well as tissue engineering study of knee.

Author contributions

All authors contributed to the conception and design of the study, analysis and interpretation of the data. Yan-long Jiang performed the calculation and Yu-tao Men drafted the article. All authors granted final approval.

Conflict of interest

None.

Acknowledgments

The project was supported by the National Natural Science Foundation of China (No. 11402171, No. 11672208 and No. 11372221) and was partly supported by the National Natural Science Key Foundation of China (No. 11432016).

References

[1] C.T. Chen, M. Bhargava, P.M. Lin, P.A. Torzilli, Time, stress, and location dependent chondrocyte death and collagen damage in cyclically loaded articular cartilage, J. Orthop. Res. 21 (2003) 888–898.
[2] L. Cui, Y. Wu, L. Cen, H. Zhou, S. Yin, G. Liu, W. Liu, Y. Cao, Repair of articular cartilage defect in non-weight bearing areas using adipose derived stem cells loaded polyglycolic acid mesh, Biomaterials 30 (2009) 2683–2693.
[3] T.K. Le, L.B. Montejano, Z. Cao, Z. Yang, D. Ang, Health care costs in US patients with and without a diagnosis of osteoarthritis, J. Pain Res. 5 (2012) 23–30.
[4] Z. Hao, H. Leng, C. Qu, C. Wan, Biomechanics of the bone and the knee joint, Guti Lixue Xuebao/Acta Mech. Solida Sin. 31 (2010) 603–612.
[5] J.R. Owen, J.S. Wayne, Influence of a superficial tangential zone over repairing cartilage defects: implications for tissue engineering, Biomech. Model. Mechanobiol. 5 (2006) 102–110.
[6] R.K. June, C.P. Neu, J.R. Barone, D.P. Fyhrie, Polymer mechanics as a model for short-term and flow-independent cartilage viscoelasticity, Mater. Sci. Eng. C 31 (2011) 781–788.
[7] C.R. Henak, E.D. Carruth, A.E. Anderson, M.D. Harris, B.J. Ellis, C.L. Peters, J.A. Weiss, Finite element predictions of cartilage contact mechanics in hips with retroverted acetabula, Osteoarthr. Cartil. 92 (2013) 1522–1529.
[8] F. Guilak, A. Ratcliffe, N. Lane, M.P. Rosenwasser, V.C. Mow, Mechanical and biochemical changes in the superficial zone of articular cartilage in canine experimental osteoarthritis, J. Orthop. Res. 12 (1994) 474–484.
[9] W. Wilson, B.C. Van, D.C. Van, P. Buma, R.B. Van, R. Huiskes, Causes of mechanically induced collagen damage in articular cartilage, J. Orthop. Res. 24 (2006) 220–228.
[10] A. Thambyah, G. Zhang, W. Kim, N.D. Broom, Impact induced failure of cartilage-on-bone following creep loading: a microstructural and fracture mechanics study, J. Mech. Behav. Biomed. 14 (2012) 239–247.
[11] S.M. Hosseini, W. Wilson, K. Ito, C.C. van Donkelaar, A numerical model to study mechanically induced initiation and progression of damage in articular cartilage, Osteoarthr. Cartil. 35 (2014) 172–191.
[12] J.T. Kaplan, C.P. Neu, H. Drissi, N.C. Emery, D.M. Pierce, Cyclic loading of human articular cartilage: the transition from compaction to fatigue, J. Mech. Behav. Biomed. 65 (2016) 734–742.
[13] K.R. Gratz, B.L. Wong, W.C. Bae, R.L. Sah, The effects of focal articular defects on cartilage contact mechanics, J. Orthop. Res. 27 (2009) 584–592.
[14] J. Desrochers, M.W. Amrein, J.R. Matyas, Viscoelasticity of the articular cartilage surface in early osteoarthritis, Osteoarthr. Cartil. 20 (2012) 413–421.

[15] L.L. Gao, X.Y. Qin, C.Q. Zhang, H. Gao, H.Y. Ge, X.Z. Zhang, Ratcheting behavior of articular cartilage under cyclic unconfined compression, Mater. Sci. Eng. C 57 (2015) 371–377.
[16] L.P. Li, J. Soulhat, M.D. Buschmann, A. Shirazi-Adl, Nonlinear analysis of cartilage in unconfined ramp compression using a fibril reinforced poroelastic model, Clin. Biomech. 14 (1999) 673–682.
[17] K. Kühn, D.D. D'Lima, S. Hashimoto, M. Lotz, Cell death in cartilage, Osteoarthr. Cartil. 12 (2004) 1–16.
[18] B.J. Ewers, D. Dvoracekdriksna, M.W. Orth, R.C. Haut, The extent of matrix damage and chondrocyte death in mechanically traumatized articular cartilage explants depends on rate of loading, J. Orthop. Res. 19 (2001) 779–784.
[19] R.W. Forsey, J. Fisher, J. Thompson, M.H. Stone, C. Bell, E. Ingham, The effect of hyaluronic acid and phospholipid based lubricants on friction within a human cartilage damage model, Biomaterials 27 (2006) 4581–4590.
[20] Q.Q. Tian, J.D. Ye, X. Li, X.K. Wang, C.Q. Zhang, L.M. Dong, Numerical simulation to the process of damage evolution of defect cartilage, Appl. Mech. Mater. 397–400 (2013) 629–632.
[21] D.D. D'Lima, S. Hashimoto, P.C. Chen, C.C. Jr, M.K. Lotz, Human chondrocyte apoptosis in response to mechanical injury, Osteoarthr. Cartil. 9 (2001) 712–719.
[22] K.E. Schlichting, T.M. Copeland-Johnson, M. Goodman, R.J. Lipert, T. Prozorov, X. Liu, T.O. Mckinley, Z. Lin, J.A. Martin, S.K. Mallapragada, Synthesis of a novel photopolymerized nanocomposite hydrogel for treatment of acute mechanical damage to cartilage, Acta Biomater. 7 (2011) 3094–3100.
[23] R. Dorotka, U. Windberger, K. Macfelda, U. Bindreiter, C. Toma, S. Nehrer, Repair of articular cartilage defects treated by microfracture and a three-dimensional collagen matrix, Biomaterials 26 (2005) 3617–3629.
[24] S.R. Oungoulian, K.M. Durney, B.K. Jones, C.S. Ahmad, C.T. Hung, G.A. Ateshian, Wear and damage of articular cartilage with friction against orthopedic implant materials, J. Biomech. 48 (2015) 1957–1964.
[25] J.S. Wayne, S.L. Woo, M.K. Kwan, Application of the u-p finite element method to the study of articular cartilage, J. Biomech. Eng. 113 (1991) 397–403.
[26] A. Vahdati, D.R. Wagner, Implant size and mechanical properties influence the failure of the adhesive bond between cartilage implants and native tissue in a finite element analysis, J. Biomech. 46 (2013) 1554–1560.
[27] E. Peña, B. Calvo, M.A. Martínez, M. Doblaré, Computer simulation of damage on distal femoral articular cartilage after meniscectomies, Comput. Biol. Med. 38 (2008) 69–81.
[28] S.M. Hosseini, Y. Wu, K. Ito, C.C. van Donkelaar, The importance of superficial collagen fibrils for the function of articular cartilage, Biomech. Model. Mechanobiol. 13 (2014) 41–51.
[29] R. Shirazi, A. Shirazi-Adl, Analysis of articular cartilage as a composite using nonlinear membrane elements for collagen fibrils, Med. Eng. Phys. 27 (2005) 827–835.
[30] M.A. Accardi, S.D. Mccullen, A. Callanan, S. Chung, P.M. Cann, M.M. Stevens, D. Dini, Effects of fiber orientation on the frictional properties and damage of regenerative articular cartilage surfaces, Tissue Eng. A 19 (2013) 2300–2310.
[31] L.L. Gao, C.Q. Zhang, L.M. Dong, Y.W. Jia, Description of depth-dependent nonlinear viscoelastic behavior for articular cartilage in unconfined compression, Mater. Sci. Eng. C 32 (2012) 119–125.
[32] F. Guilak, L.A. Setton, Functional Tissue Engineering and the Role of Biomechanical Signaling in Articular Cartilage Repair, Springer, 2003.
[33] S.M. Hosseini, M.B. Veldink, W. Wilson, K. Ito, C.C.V. Donkelaar, Collagen fibril damage is not the cause of early softening in articular cartilage, J. Biomech. 45 (2011) S166.
[34] C.Q. Zhang, L.L. Gao, L.M. Dong, H.Y. Liu, Depth-dependent normal strain of articular cartilage under sliding load by the optimized digital image correlation technique, Mater. Sci. Eng. C 32 (2012) 2390–2395.
[35] W. Wilson, C.C.V. Donkelaar, B.V. Rietbergen, K. Ito, R. Huiskes, Stresses in the local collagen network of articular cartilage: a poroviscoelastic fibril-reinforced finite element study, J. Biomech. 37 (2004) 357–366.
[36] S. Chegini, S.J. Ferguson, Time and depth dependent Poisson's ratio of cartilage explained by an inhomogeneous orthotropic fiber embedded biphasic model, J. Biomech. 43 (2010) 1660–1666.
[37] K. Boettcher, S. Kienle, J. Nachtsheim, R. Burgkart, T. Hugel, O. Lieleg, The structure and mechanical properties of articular cartilage are highly resilient towards transient dehydration, Acta Biomater. 29 (2015) 180–187.
[38] S. Federico, A. Grillo, R.G. La, G. Giaquinta, W. Herzog, A transversely isotropic, transversely homogeneous microstructural-statistical model of articular cartilage, J. Biomech. 38 (2005) 2008–2018.
[39] A. Seifzadeh, D.C.D. Oguamanam, N. Trutiak, M. Hurtig, M. Papini, Determination of nonlinear fibre-reinforced biphasic poroviscoelastic constitutive parameters of articular cartilage using stress relaxation indentation testing and an optimizing finite element analysis, Comput. Methods Prog. Biomed. 107 (2012) 315–326.
[40] F. Richard, M. Villars, S. Thibaud, Viscoelastic modeling and quantitative experimental characterization of normal and osteoarthritic human articular cartilage using indentation, J. Mech. Behav. Biomed. 24 (2014) 41–52.
[41] N.S. Landinez-Parra, D.A. Garzón-Alvarado, J.C. Vanegas-Acosta, A phenomenological mathematical model of the articular cartilage damage, Comput. Methods Prog. Biomed. 104 (2011) 58–74.
[42] V. Klika, E.A. Gaffney, Y.C. Chen, C.P. Brown, An overview of multiphase cartilage mechanical modelling and its role in understanding function and pathology, J. Mech. Behav. Biomed. 62 (2016) 139–157.
[43] N. Sakai, Y. Hagihara, T. Furusawa, N. Hosoda, Y. Sawae, T. Murakami, Analysis of biphasic lubrication of articular cartilage loaded by cylindrical indenter, Tribol. Int. 46 (2012) 225–236.
[44] N. Sakai, C. Hashimoto, S. Yarimitsu, Y. Sawae, M. Komori, T. Murakami, A functional effect of the superficial mechanical properties of articular cartilage as a load bearing system in a sliding condition, Biosurf. Biotribol. 2 (2016) 26–39.
[45] M. Adouni, Y.Y. Dhaher, A multi-scale elasto-plastic model of articular cartilage, J. Biomech. 49 (2016) 2891–2898.
[46] J.M. Deneweth, S.G. Mclean, E.M. Arruda, Evaluation of hyperelastic models for the non-linear and non-uniform high strain-rate mechanics of tibial cartilage, J. Biomech. 46 (2013) 1604–1610.
[47] Q. Meng, S. An, R.A. Damion, Z. Jin, R. Wilcox, J. Fisher, A. Jones, The effect of collagen fibril orientation on the biphasic mechanics of articular cartilage, J. Mech. Behav. Biomed. 65 (2016) 439–453.
[48] M. Taffetani, M. Griebel, D. Gastaldi, S.M. Klisch, P. Vena, Poroviscoelastic finite element model including continuous fiber distribution for the simulation of nanoindentation tests on articular cartilage, J. Mech. Behav. Biomed. 32 (2014) 17–30.
[49] G.A. Ateshian, V. Rajan, N.O. Chahine, C.E. Canal, C.T. Hung, Modeling the matrix of articular cartilage using a continuous fiber angular distribution predicts many observed phenomena, J. Biomech. Eng. 131 (2009) 138–140.
[50] Y. Al-Saffar, B. Murphy, W. Herzog, Deformation patterns of cracked articular cartilage under compression, Osteoarthr. Cartil. 22 (2014) S373–S374.
[51] T.S. Atkinson, R.C. Haut, N.J. Altiero, An investigation of biphasic failure criteria for impact-induced fissuring of articular cartilage, J. Biomech. Eng. 120 (1998) 536–537.
[52] C.B. Raub, S.C. Hsu, E.F. Chan, R. Shirazi, A.C. Chen, E. Chnari, E.J. Semler, R.L. Sah, Microstructural remodeling of articular cartilage following defect repair by osteochondral autograft transfer, Osteoarthr. Cartil. 21 (2013) 860–868.
[53] D.C. Flanigan, J.D. Harris, P.M. Brockmeier, R.L. Lathrop, R.A. Siston, The effects of defect size, orientation, and location on subchondral bone contact in oval-shaped experimental articular cartilage defects in a bovine knee model, Knee Surg. Sports Traumatol. 22 (2012) 174–180.
[54] R.F. Moyer, A. Ratneswaran, F. Beier, T.B. Birmingham, Osteoarthritis year in review 2014: mechanics - basic and clinical studies in osteoarthritis, Osteoarthr. Cartil. 22 (2014) 1989–2002.
[55] C. Zhang, Y.Z. Cai, X.J. Lin, One-step cartilage repair technique as a next generation of cell therapy for cartilage defects: biological characteristics, preclinical application, surgical techniques, and clinical developments, Arthroscopy 32 (2016) 1444–1450.